Talanta 97 (2012) 406–413

Contents lists available at SciVerse ScienceDirect

Talanta

journal homepage: www.elsevier.com/locate/talanta

Conjugates of graphene oxide covalently linked ligands and gold nanoparticles to construct silver ion graphene paste electrode

Chunli Yang, Yaqin Chai *, Ruo Yuan, Wenju Xu, Ting Zhang, Feng Jia

Key Laboratory of Eco-environments in Three Gorges Reservoir Region, Ministry of Education, School of Chemistry and Chemical Engineering, Southwest University, Chongqing 400715, PR China

ARTICLE INFO

Article history:
Received 4 April 2012
Accepted 27 April 2012
Available online 8 May 2012

Keywords:
Graphene paste electrode
Graphene oxide
Silver
Potentiometric

ABSTRACT

We reported on the synthesis and application of ionophore–gold nanoparticle conjugates in Ag^+ graphene paste electrode. Ionophore was a novel graphene oxide nanosheets (NGO) covalently grafted 2-thiophenecarboxylic (TPC) hybrid material. The hybrid material NGO–TPC decorated with gold nanoparticles was used as both a receptor and an ion-to-electron transducer to fabricate Ag^+ graphene paste electrode. The developed electrode was highly selective to Ag^+ over other tested cations and exhibited an excellent Nernstian slope of 59.3 mV dec^{-1} ranging from 8.4×10^{-7} to $1.0\times10^{-}$ M with a detection limit of 6.3×10^{-7} M. Moreover, it also showed a fast response time and a long lifetime. Importantly, the new method of immobilizing ligands on NGO nanosheets to construct electrode successfully solved the universal problem of the electrode components loss from ion-selective electrode.

1. Introduction

The focus of ion-selective electrodes (ISEs) research has been redirected from liquid contact ISEs toward solid contact ion-selective electrodes (SC-ISEs) during recent years [1]. Nowadays, SC-ISEs are recognized as the most promising potentiometric sensors because of their excellent analytical performance, such as robustness and easy handling. And the most important aspect for SC-ISEs is that solid material transducers can reversibly and efficiently convert a chemical event into an electronic signal [2]. Conducting polymers as the traditional transducers are often introduced into the polymeric membrane with non-covalent bond form, which results in improving stability and lower impedance in comparison with coated wire electrodes [3–5]. Several types of carbon nanotubes have also been used as ion-to-electron transducers in SC-ISEs due to their special physicochemical properties, such as high surface-to-volume ratio and high electrical conductivity [6–10]. Compared with conducting polymers and carbon nanotubes, graphene, an atomical layer of sp^2 carbon atoms in a densely packed honeycomb two-dimensional lattice, possesses a much larger surface area of 2630 $m^2\,g^{-1}$ and excellent electrical conductivity of 7200 S m^{-1} [11]. And it has been substantially applied in the areas of electrochemical sensors [12–15]. But, to the best of our knowledge, the application of graphene hybrid material in the fabrication of potentiometric sensors has not been reported before.

In recent years, gold nanoparticles (Au NPs) have gained significant popularity as membrane materials in ISEs, because they can remarkably improve sensitivity, selectivity and potentiometric stability of the sensors. In general, there are two alternative reported approaches for the use of Au NPs in ISEs. One is that Au NPs are used as solid contact layers by dropping Au NPs solution on the prepared electrodes [16]. The other is that ligands containing the –SH radical are immobilized on Au NPs [17–19]. However, these approaches are still awkward to construct ISEs. In the first approach, the recognition and transduction events are divided into two layers in the electrodes. In the second approach, the selection of the ligands is restricted, which must contain –SH radical in their structures.

The leaching of membrane components affects potentiometric stability and contaminates test sample, which is seen as a serious problem for potentiometric sensors. To solve this problem, earlier efforts have been made by the covalent immobilization of the ionophore on the functional groups of the polymeric membrane [20] or the covalent linkage of the ionophore to gold nanoparticles [21]. Nevertheless, these approaches require compromise of the sensitivity and selectivity of the potentiometric sensors [2].

For the first time, we reported on the synthesis and analytical application of ionophore–gold nanoparticle conjugates (NGO–AuNP–TPC) with both recognition and transduction properties in solid Ag^+ graphene paste electrode (GPE). Graphene hybrids (NGO–TPC) were obtained by ligands TPC covalently linking to

* Corresponding author. Tel.: +86 23 6825 2277; fax: +86 23 6825 3172.
E-mail address: yqchai@swu.edu.cn (Y. Chai).

0039-9140/$ - see front matter © 2012 Elsevier B.V. All rights reserved.
http://dx.doi.org/10.1016/j.talanta.2012.04.053

graphene oxide nanosheets (NGO). This new approach of immobilizing ligands on planar sheet NGO can overcome the problem of ligands leaching from GPE and further improve the sensitivity and selectivity of the potentiometric sensors. Gold nanoparticles (Au NPs), because of their fascinating optical and surface properties for catalytic and nanotechnology applications, were loaded onto the NGO–TPC nanosheets to obtain NGO–AuNP–TPC. The advantages of this novel method were as follows: (i) NGO–AuNP–TPC can be used as an integrated ionophore-transducer material in Ag^+ GPE. (ii) The selection of ligands was not restricted. (iii) The performance characteristics of the electrode were also substantially improved.

2. Experimental

2.1. Apparatus and reagents

Potentiometric measurements were performed with a MP230 pH meter (Metter Toledo, Switzerland) and a pHS-3C digital ion analyzer (Shanghai Dazhong Analytical Instruments, Shanghai, China). The AC impedance was recorded with an impedance measurement unit (IM6e, ZAHNER elektrick Co., Germany) and the frequency range used was 10^{-2}–10^{6} Hz (25 °C). UV–visible absorption spectra were obtained on a UV/vis spectrophotometer (Lambda 17, Perkin-Elmer, USA). IR spectra of three ionophores were recorded with a Spectrum GX FTIR instrument (Mattson RK-6000, USA). FT-Raman spectra were recorded using a Nd-YAG laser, at wavelength 1064 nm, power 200 mW and a germanium diode detector (RFS-100/ S, Bruker Co., Germany). The surface morphologies of graphene materials were identified by the scanning electron microscope (SEM, S-4800, Hitachi, Tokyo, Japan) Atomic force microscopy (AFM) images were taken using scanning probe microscope (Veeco, USA).

Graphene Oxide, 1-(3-Dimethylaminopropyl)-3-ethylcarbodiimide hydrochloride (EDC), N-Hydroxy succinimide (NHS) and 2-thiophenecarboxylic were bought from Sigma Chemical Co. (St.Louis, MO, USA). NaOH was purchased from Chengdu organic chemicals Co. Ltd. of the Chinese Academy of Science. Nitric acid was purchased from Chongqing chemicals (Chongqing, China). Reagent grade paraffin oil, graphite powder, chloroacetic acid and the nitrate salts of the used cations were purchased from Shanghai Chemicals (Shanghai, China). All of the chemicals used were of analytical-reagent grade. All aqueous solutions were prepared with deionized distilled water.

2.2. Preparation of ionophore–gold nanoparticle conjugates

We developed a simple route to prepare the ionophore–gold nanoparticle conjugates NGO–AuNP–TPC (Fig. 1). The preparation process of NGO–AuNP–TPC was as follows.

For the preparation of nanoscale graphene oxide (NGO): 100 mg of GO and 50 mL of deionized distilled water were mixed in a bath, and then the bath was sonicated for 1 h, obtaining a clear NGO solution (2 mg/mL) [22].

The conjugation of TPC with NGO: Firstly, to increase the amount of –COOH groups on the surface of NGO, –OH groups on the NGO sheets were converted to –COOH groups via conjugation of acetic acid moieties of chloroacetic acid using the method reported by Sun et al. [23]. Second, TPC conjugated with NGO–COOH by reaction between the –COOH groups from the NGO–COOH and $–NH_2$ groups from the TPC molecules.

NaOH (12 g) and chloroacetic acid (10 g) were added to the above NGO suspension and the bath was sonicated for 3 h to convert the –OH groups into -COONa groups. NGO–COOH, the resulting product, was obtained through adding dilute nitric acid and purified by repeated rinsing and centrifugation with deionized water. After that, all of the NGO–COOH was added to water/ethanol (1:1, v/v) mixture solution. NHS (182.5 mg) and EDC (125 mg) were added to the above NGO–COOH suspension (10 mL), and the mixture was treated by ultrasonication for 2 h. 300 mg of TPC were added and the mixture was stirred overnight. The unreacted materials were separated out by repeated rinsing and centrifugation with water/ethanol (1:1, v/v) mixture solution. The final products, so-called ionophore (NGO–TPC), were obtained.

Preparation of ionophore–gold nanoparticle conjugates (NGO–AuNP–TPC): Gold nanoparticles (Au NPs) with mean size of 16 nm

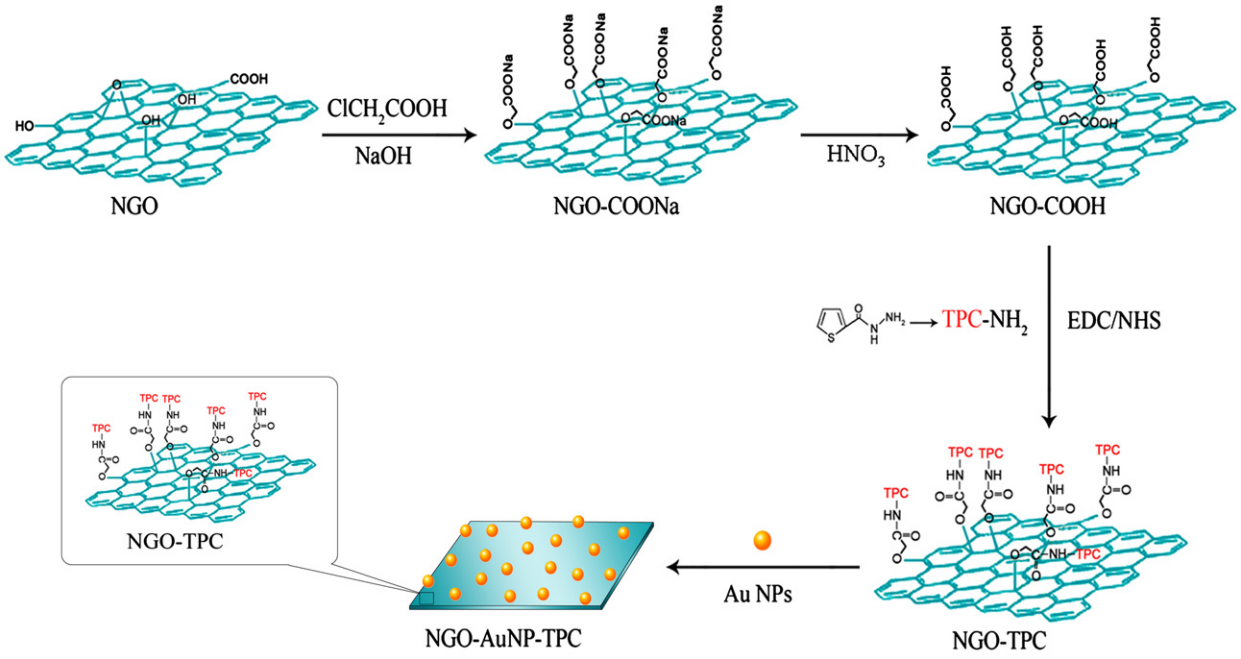

Fig. 1. Schematic representation of the preparation procedure for NGO–AuNP–TPC.

(the graph not shown) were prepared by reducing gold chloride tetrahydrate with sodium citrate at 100 °C for half an hour [24]. Then, to prepare the Au NP-decorated NGO–TPC, the aqueous dispersion of Au NPs (2 mL) was mixed with the aqueous dispersion of 50 mg GO–TPC under sonication for 30 min, and the mixture solution was stirred overnight. After five cycles of washing with a water/ethanol (1:1, v/v) mixture and centrifugation to remove the free Au NPs, the integrated ionophore-transducer material NGO–AuNP–TPC was obtained [25].

2.3. Preparation of graphene paste electrode

The graphene paste electrodes (GPEs) were prepared by thoroughly hand-mixing NGO–AuNP–TPC, graphite powder and paraffin oil. The homogeneous paste was carefully packed into the end of a disposable polyethylene syringe (diameter of 3 mm and 3 cm in length) and intensively pressed by using glass rod to avoid possible air gaps that often enhance the electrode resistance. A copper wire was inserted into the opposite end to establish electrical contact. The electrode surface was polished on a soft paper until the surface had a shiny appearance. A new surface can be obtained by scrapping out the old surface. The electrodes were finally conditioned for 24 h in HNO_3 solution (pH 3.0).

2.4. EMF measurements

EMF measurements were performed through a digital ion analyzer Model pHS-3C at room temperature. A double junction saturated calomel electrode was used as the reference electrode for the Ag^+-measurements. The galvanic cell can be represented as follows:

$Hg–Hg_2Cl_2$, KC1 (satd.)|1.0 M KNO_3|test solution||graphene paste electrode|Cu

The activities of metal ions were calculated according to the Debye–Hückel equation [26].

3. Results and discussion

3.1. Characteristics of ionophore–gold nanoparticle conjugates

Morphological information of the NGO and the NGO–AuNP–TPC was observed by atomic force microscopy (AFM) and scanning electron microscope (SEM) images (Fig. 2). Fig. 2a and c show the AFM and SEM images of NGO, respectively. Fig. 2d shows the SEM image of the NGO–AuNP–TPC nanosheets obtained from an aqueous dispersion. Obviously, the Au NPs were successfully loaded onto the NGO–TPC nanosheets. Sphere-like or particles-like nanostructures distributed on the surface or edge of NGO–TPC nanosheets in the AFM image of NGO–AuNP–TPC (Fig. 2b), which further indicated that the Au NPs were decorated on NGO–TPC nanosheets.

The conjugation of TPC with NGO–COOH was confirmed by UV/vis and FTIR measurements. In the UV/vis spectra (Fig. 3a), the peak of NGO disappears at 232 nm, while a new peak at 245 nm appears due to the conjugation of TPC with NGO–COOH. An obvious peak at 1593 cm^{-1} in the FTIR spectrum indicates the presence of thiophene ring in NGO–TPC (Fig. 3b) [27]. Fig. 3c shows the Raman spectra of NGO, NGO–COOH, NGO–TPC and NGO–AuNP–TPC. The Raman spectrum corresponding to the functionalized graphene was very similar to that of raw NGO. The spectra show the carbon D and G band peaks at ~1310 cm^{-1} and ~1600 cm^{-1}, respectively, which is in agreement with that reported in literature [28]. It is notable that the intensity ratios

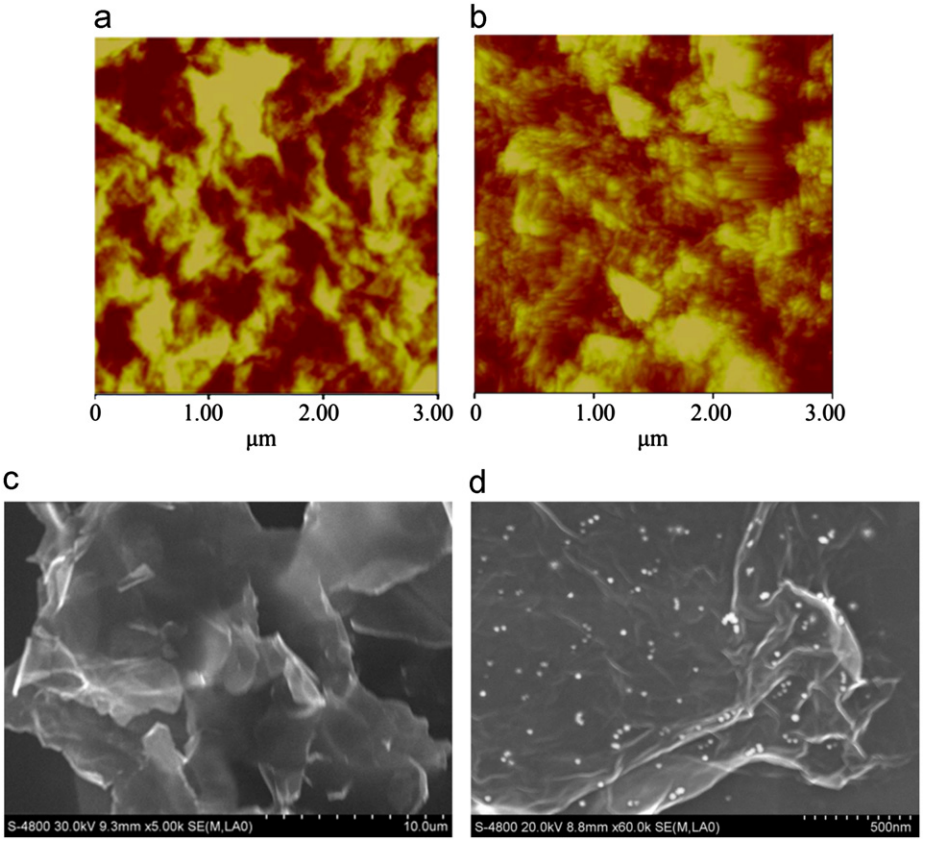

Fig. 2. AFM images of the (a) NGO and (b) NGO–AuNP–TPC nanosheets, SEM images of the (c) NGO and (d) NGO–AuNP–TPC nanosheets.

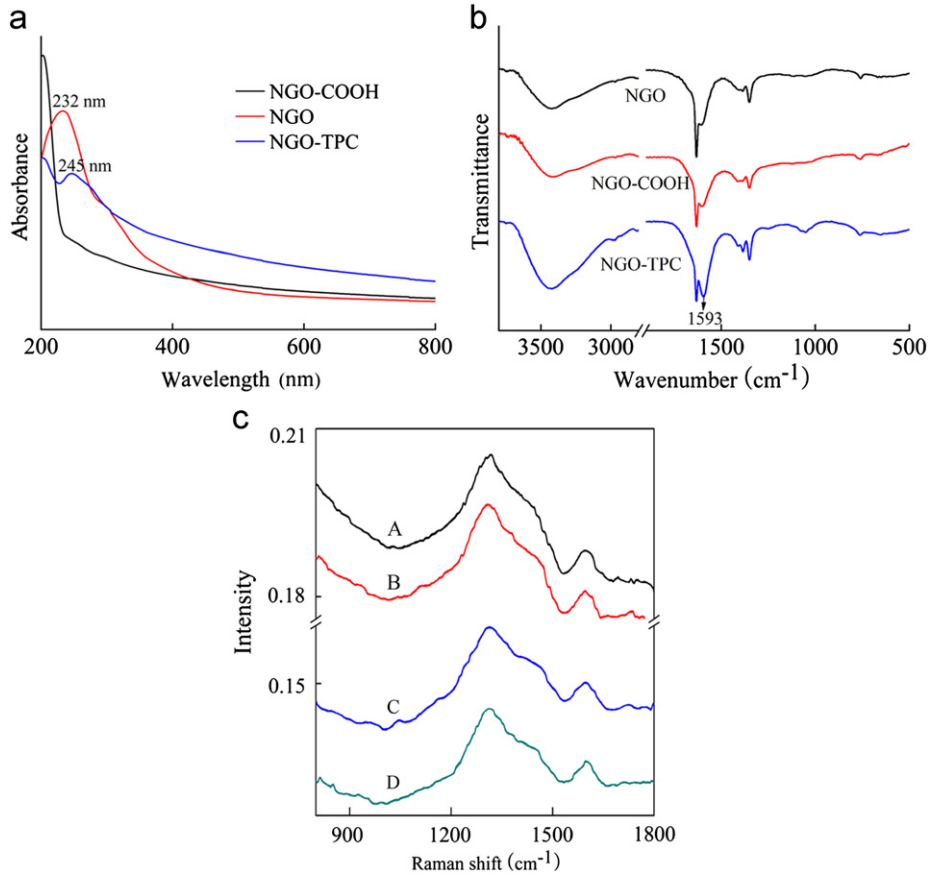

Fig. 3. (a) UV/vis spectra of the NGO, NGO–COOH and NGO–AuNP–TPC in aqueous solution, (b) FT-IR spectra of the NGO, NGO–COOH and NGO–TPC measured in KBr pellets, (c) Raman spectra of NGO (A), NGO–COOH (B), NGO–TPC (C) and NGO–AuNP–TPC (D).

D/G from NGO to NGO–AuNP–TPC display slight differences (1.093; 1.083; 1.072; 1.071 for raw NGO, NGO–COOH, NGO–TPC and NGO–AuNP–TPC respectively). The ID/IG ratio of the NGO–COOH was smaller than that of the pristine NGO, indicating that preparation of NGO–COOH had no detrimental effect on the structure of pristine NGO. Rather, converting the hydroxyl, epoxide, and ester groups of the NGO into the –COOH groups improved the original defect sites on the surface of the pristine NGO. The ID/IG ratios of the NGO–TPC and NGO–AuNP–TPC were almost same, indicating that decoration of the NGO–TPC nanosheets with Au NPs had no detrimental effect on the structure of NGO–TPC.

3.2. Composition and potential response characteristics of the GPE

Prior to experiments, various NGO–AuNP–TPC GPEs were prepared and electrode No. 3 (Table 1) was used for the detection of different cations (Fig. 4a and b). As can be seen, the developed electrode exhibited a Nernstian behavior and the most sensitive response toward Ag^+ among different tested cations. Hence, NGO–AuNP–TPC was selected as the integrated ionophore-transducer material for the fabrication of Ag^+ GPE. It is well known that the sensitivity and linearity of the electrode significantly depend on the amount of ionophore in the electrode composition [29–31]. Thus, the effect of the percent of NGO–AuNP–TPC in the paste composition on the potential response of GPE was investigated (Table 1). The results suggested that the electrode with composition of NGO–AuNP–TPC/graphite powder/paraffin oil in (w/w, %) 6.3/65.1/28.6 (No. 3) exhibited higher sensitivity (slope: 59.3 mV dec^{-1}), wider linear range (8.4×10^{-7} to 1.0×10^{-1} M) and lower detection limit (6.3×10^{-7} M) than others. The electrode without NGO–AuNP–TPC showed a very small response to Ag^+, it was probably due to the sorption of a small amount of Ag^+ on the electrode surface, and the small response can be neglected. Therefore, the No. 3 electrode was selected as the optimal electrode composition in the further experiments.

3.3. Effect of pH on electrode performance

In order to investigate the pH effect on the potential response of the electrode, the NGO–AuNP–TPC GPE was tested at two Ag^+ concentrations (1.0×10^{-2} and 1.0×10^{-3} M) over the pH range between 1.0 and 11.0 (adjusted with HNO_3 and NaOH). It is clear from Fig. 5 that the potential plateau appears in a pH range from 3.0 to 9.0, beyond which a gradual change in potential is observed. At pH higher than 9.0, the decreased potential seemed ascribable to the formation of some hydroxy complexes of Ag^+ ion in solution [32]. While the potential cannot keep constant at $pH<3$, this may be the high concentration of H^+ that can exchange with Ag^+ adsorbed on the NGO–AuNP–TPC molecules [33,34]. It was concluded that pH range 3.0–9.0 was a suitable working range for Ag^+ NGO–AuNP–TPC GPE.

3.4. Electrode selectivity

In this context, the unbiased potentiometric selectivity coefficients were measured by the separate solution method (SSM) according to IUPAC recommendations [35–38]. The resulting values of potentiometric selectivity coefficients for the NGO–AuNP–TPC GPE are shown in Table 2. It reveals that the electrode exhibits fairly high selectivity towards Ag^+ ion over a large number of other cations.

Table 1
Optimization of membrane ingredients of NGO–AuNP–TPC GPE.

No.	Composition (%)			Electrode characteristics		
	Carrier	GP	PO	Slope (mV dec^{-1})	LR (M)	DL (M)
1	–	71.4	28.6	–	–	–
2	4.7	69.5	25.8	57.0	1.7×10^{-5}–1.0×10^{-1}	1.0×10^{-5}
3	6.3	65.1	28.6	59.3	8.4×10^{-7}–1.0×10^{-1}	6.3×10^{-7}
4	7.4	65.4	27.2	64.8	7.4×10^{-6}–1.0×10^{-1}	5.0×10^{-6}
5	8.9	65.4	25.7	64.9	5.2×10^{-5}–1.0×10^{-1}	3.1×10^{-5}

GP: graphite powder, PO: paraffin oil, LR: linear range, DL: detection limit, Carrier: NGO–AuNP–TPC.

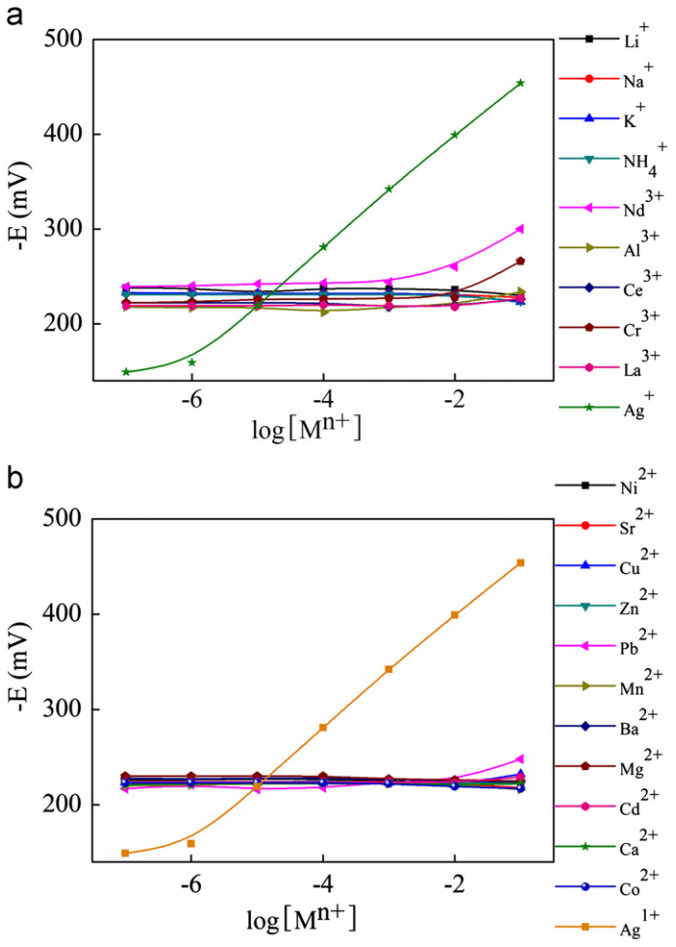

Fig. 4. Potential responses of NGO–AuNP–TPC GPE for different metal ions (a and b).

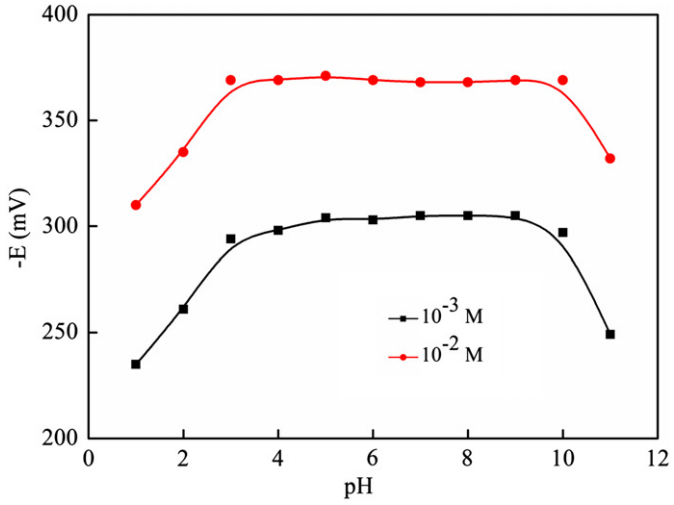

Fig. 5. pH effect of the test solution on the potential response of the Ag^+ NGO–AuNP–TPC GPE.

Table 2
Selectivity coefficients of various interfering cations based on NGO–AuNP–TPC GPE.

Interfering ion	$LogK^{pot}_{Ag^+,J}$	Interfering ion	$LogK^{pot}_{Ag^+,J}$
Na^+	−5.19	Co^{2+}	−5.59
K^+	−5.32	Ni^{2+}	−5.69
Li^+	−5.36	Sr^{2+}	−5.71
NH_4^+	−5.24	Mn^{2+}	−5.68
Ba^{2+}	−5.69	Cu^{2+}	−5.54
Cd^{2+}	−5.54	Cr^{3+}	−5.05
Ca^{2+}	−5.63	Ce^{3+}	−5.75
Mg^{2+}	−5.71	Al^{3+}	−5.56
Pb^{2+}	−5.71	La^{3+}	−5.64
Zn^{2+}	−5.63		

The other two GPEs were prepared to compare potentiometric selectivity coefficients of four interference ions (Li^+, Cu^{2+}, Sr^{2+}, La^{3+}). The preparation of NGO–TPC GPE was similar to that of NGO–AuNP–TPC GPE, except that NGO–TPC was used instead of NGO–AuNP–TPC. Free receptor GPE (NGO+TPC GPE) was prepared by NGO and TPC instead of NGO–AuNP–TPC. The potentiometric selectivity coefficients of three GPEs were compared and the result showed in Fig. 6. It was obviously seen that the selectivity coefficients dramatically increased by two to three logarithmic orders of magnitude when the NGO–TPC was used instead of NGO and TPC in GPE. The grafting of TPC on the NGO is mainly localized at the surface of functionalized graphene, so the ligand molecules are close to each other. This is benefit for the formation of sandwich complexes between two ligand molecules and the silver ion. This specific configuration, in which ligands covalently linked to functionalized graphene, maybe impress selectivity coefficients for the reported ion. Moreover, the selectivity coefficients for NGO–AuNP–TPC GPE are higher than those for NGO–TPC GPE without Au NPs. Hence, Au NPs decorated on the surface of NGO–AuNP–TPC nanosheets can also improve selectivity of the electrode.

The effect of common sample matrix components on the electrode's potential responses was also investigated. The cell potentials of silver nitrate and silver sulfate were obtained in the same condition, respectively. No significant changes in the EMF versus log[Ag^+] plots were observed, indicating that these anions (NO_3^- and SO_4^{2-}) did not cause any interference.

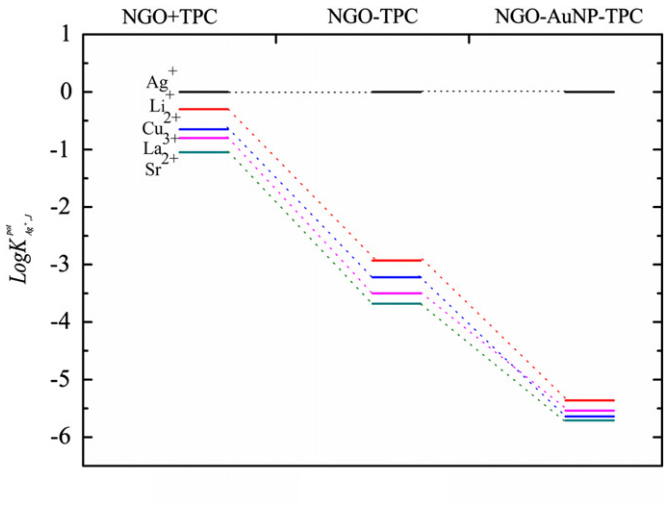

Fig. 6. Potentiometric selectivity coefficients of Ag^+ GPEs determined by the SSM. The first column shows free receptor GPE, the second column the NGO–TPC GPE and the third column the NGO–AuNP–TPC GPE.

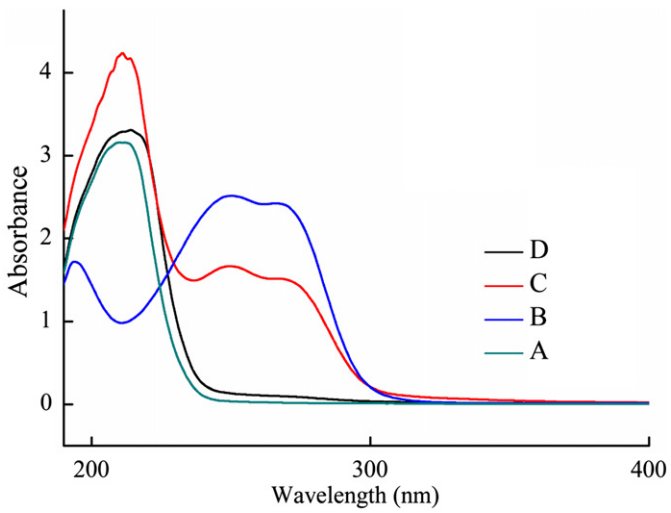

Fig. 8. UV–visible spectra: (A) pH 3.0 HNO_3 solution, (B) aqueous solution of TPC, (C) conditioning solutions of free receptor GPE in pH 3.0 HNO_3 for 7 days and (D) conditioning solutions of NGO–AuNP–TPC GPE in pH 3.0 HNO_3 for 7 days.

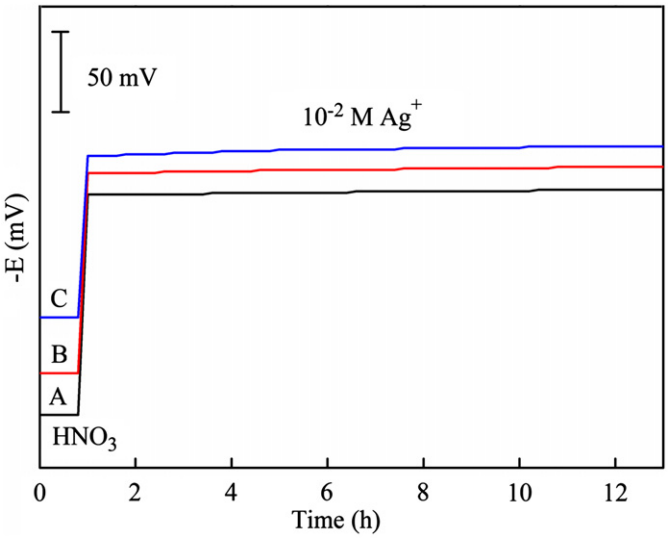

Fig. 7. Potential stability of the three different GPEs over 13 h for an change from pH 3.0 HNO_3 solution to 10^{-2} M Ag^+ solution, (A) NGO–AuNP–TPC GPE, (B) NGO–TPC GPE and (C) free receptor GPE.

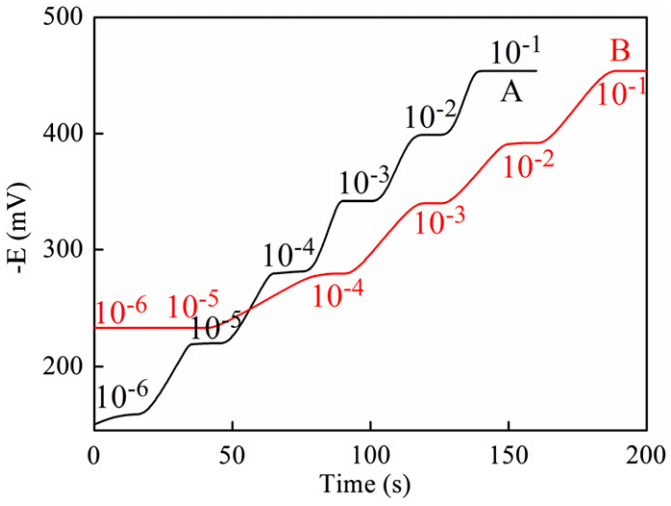

Fig. 9. Dynamic response time of the Ag^+ GPE. (A) NGO–TPC GPE and (B) NGO–AuNP–TPC GPE.

3.5. *Stability of GPE and diffusion property analysis of ionophore–gold nanoparticle conjugates from the GPE.*

The potential stability was evaluated by measuring the EMF for 12 h using a 10^{-2} M Ag^+ solution (Fig. 7). Standard deviation (SD) of potential readings for the NGO–AuNP–TPC GPE was 1.05 mV (n=60), which was similar to that of the NGO–TPC GPE (1.20 mV). In contrast, the SD of the potential stability for the free receptor GPE was almost twice as much (SD=1.87 mV), confirming the increase of the stability for the NGO–AuNP–TPC GPE. The increased stability observed for the NGO–AuNP–TPC GPE with respect to the NGO+TPC GPE was related to the loss of the GPE components. The presence of leaching components for the free receptor GPE was evidenced by UV–visible spectra (Fig. 8). The NGO–AuNP–TPC GPE and free receptor GPE were conditioned in HNO_3 solution for 7 days (pH 3.0), respectively. Their conditioning solutions were used for UV–visible spectra analysis. The UV–vis spectrum of conditioning solution for NGO–AuNP–TPC GPE showed one peak (line D) at the same wavelength of HNO_3 solution (line A). But other two peaks in the UV–vis spectrum of conditioning solution for free receptor GPE (line C) may attribute to TPC (line B). This proved that ligand molecules TPC leached out from the free receptor GPE, in which ligands TPC were not immobilizied on the NGO nanosheets. On the contrary, the components in NGO–AuNP–TPC GPE were not lost, because the TPC molecules were covalently linked to NGO nanosheets.

3.6. *Dynamic response time, reproducibility and lifetime*

Dynamic response time is an important factor for ion selective electrode. In this report, the response times of the NGO–AuNP–TPC GPE and NGO–TPC GPE were recorded by measuring a serious of Ag^+ solutions from 1.0×10^{-6} to 1.0×10^{-1} M, respectively. Fig. 9 clearly indicates that the potentiometric response time of the NGO–AuNP–TPC GPE (10 s) is faster than that of the NGO–TPC

GPE (22 s). This may be the decoration of Au NPs which can enhance the membrane conductivity. In order to evaluate the reproducibility of GPE, the NGO–AuNP–TPC GPE dipped alternatively into Ag^+ ion solutions of 1.0×10^{-3} M and 1.0×10^{-2} M demonstrated a SD of 0.73 mV ($n=12$) over 2 h. We periodically recalibrated the potentiometric response to Ag^+ ion in standard silver nitrate solutions. The electrode could be used for at least 3 months without any divergence. Moreover, the lifetime of the electrode was also studied in a lake water sample. The electrode was repeatedly tested 10 times a day over half month, the potential of the water sample did not change significantly and the SD was 1.39 mV ($n=150$). It indicates that the electrode exhibits fast response time, good reversibility and long lifetime.

3.7. Comparison of the response characteristics of different Ag^+ GPE

Potential response characteristics of different Ag^+ GPEs were compared. As can be seen in Table 3, GPE based on matrix (NGO–COOH) did not exhibit a Nernstian response to Ag^+. And shiny surface of the electrode was broke during the experiment. This may be that the matrix was hydrophilic material. The NGO–AuNP–TPC GPE showed a closer to Nernstian slope (59.3 mV dec^{-1}) and wider linear range with lower detection limit than those of NGO–TPC GPE. This result indicated that Au NPs on NGO–AuNP–TPC nanosheets can remarkably improve sensitivity, linear range and detection limit of Ag^+ GPE.

3.8. Impedance characterization

The electrochemical characterizations of NGO–TPC GPE and NGO–AuNP–TPC GPE were performed by electrochemical impedance spectroscopy (EIS Fig. 10a and b). The EIS measurements were operated at open-circuit with amplitude of 25 mV and a frequency range from10^{-2} to 10^6 Hz. The high-frequency semicircle was related to the bulk impedance of the membrane, and Warburg impedance was observed at the low frequency. As can be seen in Fig. 10a and b, the bulk resistance of the NGO–TPC GPE decreases with the increasing of Ag^+ concentration, the change of bulk resistance for NGO–AuNP–TPC GPE is the same as that of NGO–TPC GPE. These results show that both NGO–TPC and NGO–AuNP–TPC could dominate Ag^+ across the membrane and the transfer process is controlled by diffusion [39]. The GPE response is attributed to the electron-exchange mechanism at the membrane–contact interface and the ion exchange at the membrane–solution interface [40].

Table 3
Comparison of the response characteristics of different Ag^+ GPE.

Electrode materials	Slope (mV dec^{-1})	LR (M)	DL (M)
NGO–COOH, 7.0 mg GP, 75.3 mg PO, 26.4 mg	–	–	–
NGO–TPC, 7.0 mg GP, 75.0 mg PO, 27.1 mg	57.3	1.4×10^{-5}–1.0×10^{-1}	1.2×10^{-5}
NGO–AuNP–TPC, 7.0 mg GP, 75.1 mg PO, 27.0 mg	59.3	8.4×10^{-7}–1.0×10^{-1}	6.3×10^{-7}

GP: graphite powder, PO: paraffin oil, LR: linear range, DL: detection limit.

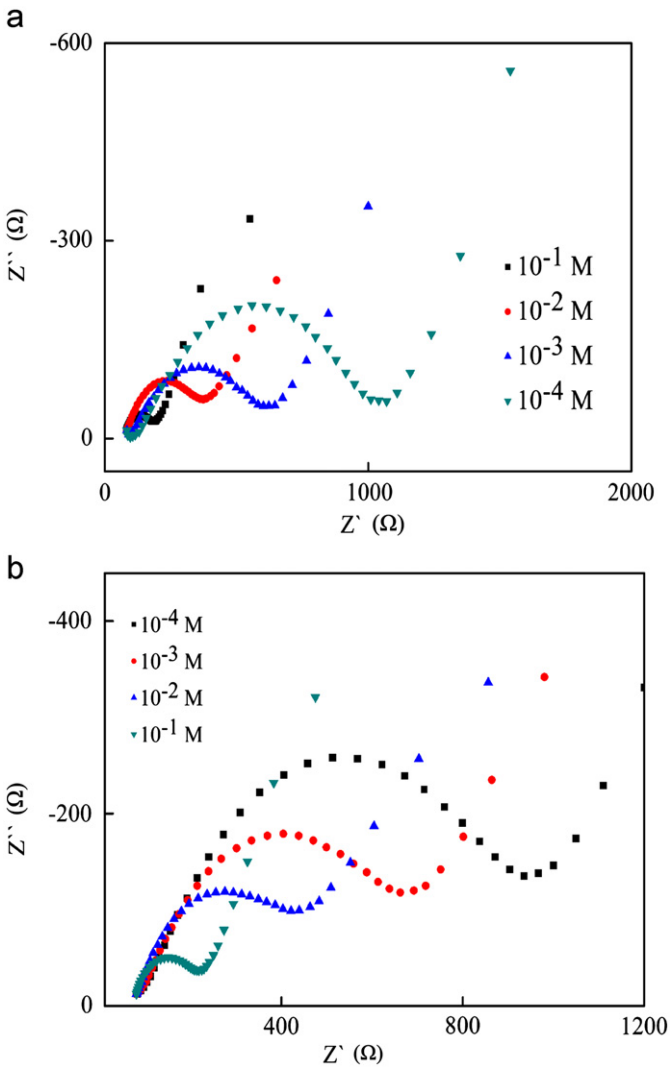

Fig. 10. Impedance plots of the (a) NGO–TPC GPE and (b) NGO–AuNP–TPC GPE in 10^{-4}–10^{-1} M Ag^+ solution.

3.9. Comparison of the different Ag^+ ion-selective electrodes

The proposed electrode was compared with recently reported electrodes (Table 4). It shows that the proposed electrode based on NGO–AuNP–TPC is superior to mostly reported silver ion selective electrodes with regard to the sensitivity, pH range, response time and selectivity. Lindfors et al. reported polyaniline nanopartice-based solid-contact silicone rubber Ag^+ electrode [1], the construction of the electrode needed extra transducer layer. In contrast, NGO–AuNP–TPC, which owned the properties of both recognition and transduction, was used as an integrated ionophore-transducer material in Ag^+ GPE for the first time. And the new method of immobilizing ligands on NGO nanosheets can solve the problem of ligands leaching from ion-selective electrodes.

4. Conclusion

In this work, graphene hybrid material was used on ion-selective electrodes (ISEs) for the first time. By using the hybrid system of immobilizing ligands on graphene nanosheets, both molecular recognition and ion-to-electron transduction in ISEs

Table 4
Comparison of the different Ag^+ ion-selective electrodes.

Electrode material Ref no.	Slope	(mV dec^{-1})	LR (M)	DL (M)	pH range	RT (s)	Log $K^{pot}_{A,B}$
Diazo-thiophenol-functionalized silica gel[a]	60.4	1.0×10^{-6}–1.0×10^{-1}	9.5×10^{-7}	4–9	50	$Li^+(-5.12)$, $Ba^{2+}(-4.88)$, $Cd^{2+}(-4.75)$, $Ca^{2+}(-4.90)$, $Mg^{2+}(-4.78)$, $Pb^{2+}(-4.83)$, $Zn^{2+}(-4.91)$, $Co^{2+}(-5.36)$, $Ni^{2+}(-4.98)$, $Sr^{2+}(-4.80)$, $Mn^{2+}(-4.67)$, $Cu^{2+}(-3.11)$, $Al^{3+}(-2.26)$, $La^{3+}(-4.35)$, $Cr^{3+}(-3.10)$, $Nd^{3+}(-3.47)$, $Ce^{3+}(-4.33)$, [e]	[41]
Dipyridyl-functionalized silica gel[a]	58.7	5.0×10^{-7}–1.0×10^{-2}	1.0×10^{-7}	3–6	<60	$K^+(-5.1)$, $Na^+(-5.2)$, $Tl^+(-3.1)$, $Ca^{2+}(-4.3)$, $La^{3+}(-3.4)$, $Ce^{3+}(-3.4)$, $Co^{3+}(-3.6)$, $Cr^{3+}(-3.5)$, $Ba^{2+}(-4.5)$, $Mg^{2+}(-4.1)$, $Fe^{2+}(-3.5)$, $Cu^{2+}(-2.5)$, $Zn^{2+}(-3.0)$, $Ni^{2+}(-3.1)$, $Pb^{2+}(-3.3)$, $Hg^{2+}(-3.2)$, $Cd^{2+}(-2.7)$,[e]	[42]
O-xylylenebis(N,N-diisobutyl dithiocarbamate) Polyaniline Nanoparticle Silicone Rubber[b]	54.7	1.0×10^{-7}–1.0×10^{-4}	–	–	–	$Na^+(-9.5)$, $K^+(-9.2)$, $Mg^{2+}(-11.1)$, $H^+(-8.6)$, $Ca^{2+}(-10.9)$, $Cu^{2+}(-8.8)$ [f]	[1]
NGO–AuNP–TPC[a]	59.3	8.4×10^{-7}–1.0×10^{-1}	6.3×10^{-7}	3–9	10	$Li^+(-5.36)$, $Na^+(-5.19)$, $K^+(-5.32)$, $NH_4^+(-5.24)$, $Sr^{2+}(-5.71)$, $Ba^{2+}(-5.69)$, $Zn^{2+}(-5.63)$, $Mn^{2+}(-5.68)$, $Ni^{2+}(-5.69)$, $Co^{2+}(-5.59)$, $Cd^{2+}(-5.54)$, $Cu^{2+}(-5.54)$, $Pb^{2+}(-5.71)$, $Mg^{2+}(-5.71)$, $Ca^{2+}(-5.63)$, $Al^{3+}(-5.56)$, $Cr^{3+}(-5.05)$, $La^{3+}(-5.64)$, $Ce^{3+}(-5.75)$[e]	

LR: linear range, DL: detection limit, RT: response time.
[a] Carbon paste electrode.
[b] Glass carbon electrode.
[e] Conventional selectivity coefficients.
[f] Unbiased selectivity coefficients.

were successfully carried out on a single material, and the problem of membrane components leaching in traditional ISEs was overcome. Gold nanoparticles loaded onto the graphene hybrids nanosheets can improve the performances of the electrode in terms of sensitivity, selectivity, detection limit and response time. Additionally, this work opens up a new route for providing a much-needed hydrophobic environment to ISEs by immobilizing hydrophilic receptors on hydrophobic material.

Acknowledgments

This work was supported by the National Natural Science Foundation of China (21075100), the National Natural Science Foundation of Chongqing City, China (CSTC–2011BA7003) and the 211 project of Southwest University (the Third Term).

References

[1] T. Lindfors, J. Szücs, F. Sundfors, R.E. Gyurcsányi, Anal. Chem. 82 (2010) 9425–9432.
[2] E.J. Parra, P. Blondeau, G.A. Crespo, F.X. Rius, Chem. Commun. 47 (2011) 2438–2440.
[3] Z. Mousavi, J. Bobacka, A. Ivaska, Electroanalysis 17 (2005) 1609–1615.
[4] K.Y. Chumbimuni-Torres, N. Rubinova, A. Radu, L.T. Kubota, E. Bakker, Anal. Chem. 78 (2006) 1318–1322.
[5] A. Kisiel, M. Mazur, S. Kuśnieruk, K. Kijewska, P. Krysiński, A. Michalska, Electrochem. Commun. 12 (2010) 1568–1571.
[6] Z. Mousavi, A. Teter, A. Lewenstam, M. Maj-Zurawska, A. Ivaska, J. Bobacka, Electroanalysis 23 (2011) 1352–1358.
[7] A. Mohadesi, Z. Motallebi, A. Salmanipour, Analyst 135 (2010) 1686–1690.
[8] M.R. Ganjali, H. Khoshsafar, F. Faridbod, A. Shirzadmehr, M. Javanbakht, P. Norouzi, Electroanalysis 12 (2009) 2175–2178.
[9] E.J. Parra, G.A. Crespo, J. Riu, A. Ruiz, F.X. Rius, Analyst 134 (2009) 1905–1910.
[10] J.X. Guo, Y.Q. Chai, R. Yuan, Z.J. Song, Z.F. Zou, Sens. Actuators B 155 (2011) 639–645.
[11] F. Li, J.J. Li, Y. Feng, L.M. Yang, Z.F. Du, Sens, Actuators B 157 (2011) 110–114.
[12] M. Pumera, A. Ambrosi, A. Bonanni, E.L.K. Chng, H.L. Poh, TrAC Trends Anal. Chem. 29 (2010) 954–965.
[13] M. Du, T. Yang, S.Y. Ma, C.Z. Zhao, K. Jiao, Anal. Chim. Acta. 690 (2011) 169–174.
[14] R. Wang, J. Sun, L. Gao, C.H. Xu, J. Zhang, Chem. Commun. 47 (2011) 8650–8652.
[15] Y.L. Yuan, X.X. Gou, R. Yuan, Y.Q. Chai, Y. Zhuo, X.Y. Ye, X.X. Gan, Biosens. Bioelectron. 26 (2011) 4236–4240.
[16] E. Jaworska, M. Wójcik, A. Kisiel, J. Mieczkowski, A. Michalska, Talanta 85 (2011) 1986–1989.
[17] A. Safavi, E. Farjami, Anal. Chim. Acta. 688 (2011) 43–48.
[18] Y.H. Yang, Z.J. Wang, M.H. Yang, M.M. Guo, Z.Y. Wu, G.L. Shen, R.Q. Yu, Sens, Actuators B 114 (2006) 1–8.
[19] M.H. Mashhadizadeha, H. Khani, A. Foroumadi, P. Sagharichi, Anal. Chim. Acta. 665 (2010) 208–214.
[20] D.N. Reinhoudt, J.F.J. Engbersen, Z. Brzozka, H.H. van der Vlekkert, G.W.N. Honig, H.A.J. Holterman, U.H. Verkerk, Anal. Chem. 66 (1994) 3618–3623.
[21] G. Jágerszki, A. Grün, I. Bitter, K. Tóth, R.E. Gyurcsányi, Chem. Commun. 46 (2010) 607–609.
[22] L.M. Zhang, J.G. Xia, Q.H. Zhao, L.W. Liu, Z.J. Zhang, Small 6 (2010) 537–544.
[23] X. Sun, Z. Liu, K. Welsher, J. Robinson, A. Goodwin, S. Zaric, H. Dai, Nano Res. 1 (2008) 203–212.
[24] Y.H. Liao, R. Yuan, Y.Q. Chai, Y. Zhuo, X. Yang, Anal. Biochem. 402 (2010) 47–53.
[25] G.L. Li, G. Liu, M. Li, D. Wan, K.G. Neoh, E.T. Kang, J. Phys. Chem. 114 (2010) 12742–12748.
[26] S. Kamata, A. Bhale, Y. Fukunaga, A. Murata, Anal. Chem. 60 (1998) 2464–2467.
[27] S.J. Howell, C.S. Day, R.E. Noftle, Inorg. Chim. Acta. 358 (2005) 3711–3723.
[28] B. Zhao, P. Liu, Y. Jiang, D.Y. Pan, H.H. Tao, J.S. Song, T. Fang, W.W. Xu, J. Power Sources 198 (2012) 423–427.
[29] M.H. Mashhadizadeha, H. Khani, A. Foroumadi, P. Sagharichi, Anal. Chim. Acta. 665 (2010) 208–214.
[30] M.H. Mashhadizadeh, E.P. Taheri, I. Sheikhshoaie, Talanta 72 (2007) 1088–1092.
[31] Y.M. Ma, R. Yuan, Y.Q. Chai, X.L. Liu, Anal Bioanal Chem. 395 (2009) 855–862.
[32] M.G. Motlagh, M.A. Taher, V. Saheb, M. Fayazi, I. Sheikhshoaie, Electrochim. Acta. 56 (2011) 5376–5385.
[33] M.R. Ganjali, F. Faridbod, P. Norouzi, M. Adib, Sens. Actuator B. 120 (2006) 119–124.
[34] M.R. Ganjali, P. Norouzi, A. Daftari, F. Faridbod, M. Salavati-Niasari, Sens. Actuator B. 120 (2007) 673–678.
[35] G. Jágerszki, Á. Takács, I. Bitter, R.E. Gyurcsányi, Angew. Chem. 50 (2011) 656–1659.
[36] E. Bakker, E. Pretsch, P. Bühlmann, Anal. Chem. 72 (2000) 1127–1133.
[37] Z. Mousavi, J. Bobacka, A. Ivaska, Electroanalysis 17 (2005) 1609–1615.
[38] Z. Szigeti, A. Malon, T. Vigassy, V. Csokai, A. Grün, K. Wygladacz, N. Ye, C. Xu, V.J. Chebny, I.B.R. Rathore, E. Bakker, E. Pretsch, Anal. Chim. Acta. 572 (2006) 1–10.
[39] A. Mcnaughtan, K. Meney, B. Grieve, Chem. Eng. 77 (2000) 17–30.
[40] V.I. Veksler, Surf. Sci. 397 (1998) 1–12.
[41] T. Zhang, Y.Q. Chai, R. Yuan, J.X. Guo, Mater. Sci. Eng. C doi: 10.1016/j.msec.2012.03.005.
[42] M. Javanbakht, M.R. Ganjali, P. Norouzi, A. Badiei, A. Hasheminasab, M. Abdouss, Electroanalysis 19 (2007) 1307–1314.